Zheng *et al.*
Chinese Journal of Mechanical Engineering (2024) 37:28
https://doi.org/10.1186/s10033-024-01010-y

Chinese Journal of Mechanical Engineering

ORIGINAL ARTICLE

Open Access

Copper-Free Resin-Based Braking Materials: A New Approach for Substituting Copper with Fly-Ash Cenospheres in Composites

Kaikui Zheng[1,2*], Youxi Lin[1*], Shanmin You[1], Zhiying Ren[1] and Jianmeng Huang[1]

Abstract

Copper particles emitted from braking have become a significant source of environmental pollution. However, copper plays a crucial role in resin-based braking materials. Developing high-performance braking materials without copper has become a significant challenge. In this paper, the resin-based braking materials were filled with fly-ash cenospheres to develop copper-free braking materials. The effects of fly-ash cenospheres on the physical properties, mechanical and friction and wear properties of braking materials were studied. Furthermore, the wear mechanism of copper-free resin-based braking materials filled with fly-ash cenospheres was discussed. The results indicate that the inclusion of fly-ash cenospheres in the braking materials improved their thermal stability, hardness and impact strength, reduced their density, effectively increased the friction coefficient at medium and high temperatures, and enhanced the heat-fade resistance of the braking materials. The inclusion of fly-ash cenospheres contributed to the formation of surface friction film during the friction process of the braking materials, and facilitated the transition of form from abrasive wear to adhesive wear. At 100–350 ℃, the friction coefficient of the optimal formulation is in the range of 0.57–0.61, and the wear rate is in the range (0.29–0.65) × 10^{-7} $cm^3 \cdot N^{-1} \cdot m^{-1}$, demonstrating excellent resistance to heat-fade and stability in friction coefficient. This research proposes the use of fly-ash cenospheres as a substitute for environmentally harmful and expensive copper in brake materials, which not only improves the performance of braking materials but also reduces their costs.

Keywords Fly-ash cenospheres, Braking materials, Friction and wear, Heat-fade resistance, Wear form

1 Introduction

Braking materials, as crucial components of various transportation vehicle braking systems, have a direct impact on the safety and reliability of people's lives and property [1]. According to the World Association of Automotive Industry, the total production of cars worldwide was over 90 million in 2023. Resin-based braking materials are currently the most widely used automotive braking materials due to their simple production process, low cost, and easy performance adjustment [2]. In recent years, research has revealed that the debris generated by braking materials during braking contains heavy metal components like zinc powder and copper powder. These components can remain suspended in the atmosphere as aerosol particles for extended periods of time. Cu-containing particles with a particle size of less than 10 μm can be deposited in the lungs of people through the respiratory system, posing a significant health risk to individuals [3–6]. In addition, copper has neurotoxic properties that can cause rapid mortality of aquatic organisms and varying degrees of pollution in

*Correspondence:
Kaikui Zheng
kuikui@fzu.edu.cn
Youxi Lin
lyx@fzu.edu.cn
[1] School of Mechanical Engineering and Automation, Fuzhou University, Fuzhou 350108, China
[2] National United Engineering Laboratory for Advanced Bearing Tribology, Henan University of Science and Technology, Luoyang 471023, China

rivers [7, 8]. Countries worldwide have gradually started to restrict the use of copper in braking materials [9, 10].

Resin-based braking materials are a multi-component composite material system consisting of various organic and inorganic components, There are more than 10–20 different formulations designed to meet various friction performance requirements, including moderate and stable friction coefficients, good heat-fade resistance and recovery, low abrasiveness on brake discs, good wear resistance, low sensitivity to braking parameters, and absence of braking noise. Numerous studies have shown that copper is an essential element in asbestos-free resin-based braking materials and plays a critical role in the tribological properties of braking materials [11]. In recent years, numerous researchers have focused on developing copper-free organic braking materials and have made significant progress. For instance, they have explored the use of stainless steel [12, 13], basalt fibers [14], special graphite [15, 16], high thermal conductivity materials [17], barite [18], and ceramic fibers [19] as alternatives to copper. However, the high-temperature frictional performance of most copper-free braking materials is not as good as that of copper-containing formulations [20]. Developing high-performance copper-free braking materials is a significant challenge for manufacturers in various countries. Fly ash is an industrial solid waste, primarily emitted by the coal-burning industry. In recent years, the production of fly ash has steadily increased. As a major coal-producing country, China annually produces up to 800 million tons of fly ash. The substantial volume of fly ash not only takes up a significant amount of land and leads to resource wastage, but also gives rise to a range of ecological problems. Currently, fly ash waste is frequently utilized in construction, agriculture, and other industries, but its comprehensive utilization rate is only about 75%. The main components of fly-ash cenospheres include SiO_2, Al_2O_3. The material has a hollow spherical structure with the lowest specific surface area [21–23]. Using it as a filler material for resin-based composites can reduce the amount of phenolic resin used in the composite. In addition, fly-ash cenospheres have favorable tribological and mechanical properties [24–26]. Utilizing them to fill braking materials not only promotes the efficient utilization of waste but also has the potential to improve the performance of braking materials.

This study utilizes fly-ash cenospheres as a filler to fabricate brake composites, substituting copper in the braking materials. The study investigates the effects of fly-ash cenospheres on the physical properties, mechanical characteristics, and frictional wear properties of the braking materials, and aims to develop an optimized formulation. The research results not only enable the high-value utilization of fly-ash cenospheres but also provide new ideas for the preparation of copper-free resin-based braking materials.

2 Experiment

2.1 Materials and Fabrication

The copper-free resin-based braking materials were filled with fly-ash cenospheres (60–80 mesh), with cashew nut shell oil-modified phenolic resin (60–100 mesh) as the binder, coir fiber (diameter of 10–20 μm, length of 15±3 mm) as the reinforcing phase, and $BaSO_4$ (325 meshes), Al_2O_3 (120 mesh), rubber (120 mesh), and graphite (100 mesh) as the remaining fillers. The braking material was prepared using a dry hot-press molding process. The preparation process is as follows: drying of raw materials → batching → mixing → hot pressing and forming → heat treatment → sample processing. The chemical composition of fly-ash cenospheres is presented in Table 1, and the surface morphology of fly-ash cenospheres is depicted in Figure 1. Table 1 indicates that the primary constituents of fly-ash cenospheres are SiO_2 and Al_2O_3. As depicted in Figure 1, the fly-ash cenospheres exhibit a spherical shape, with a rough microscopic surface that enhances their adhesion to the resin.

2.2 Test Method

2.2.1 Single-Factor Experiment

To study the effect of fly-ash cenospheres content on braking material performance, the content of fly-ash cenospheres in the braking material was varied from 0% to 25%, as detailed in Table 2.

2.2.2 Formula Optimization

The braking material formulation was optimized using orthogonal experiments to analyze the impact of the interaction between fly-ash cenospheres, resin, coir fiber, and Al_2O_3, as well as the interaction between components, on the wear rate and friction coefficient of the sample, and to obtain the optimal formulation. In

Table 1 Composition of fly-ash cenospheres (mass fraction, %)

Composition	SiO_2	Al_2O_3	Fe_2O_3	CaO	MgO	K_2O	Na_2O	Others
Content	53.2	37.71	4.18	0.07	2.63	1.24	0.30	0.67

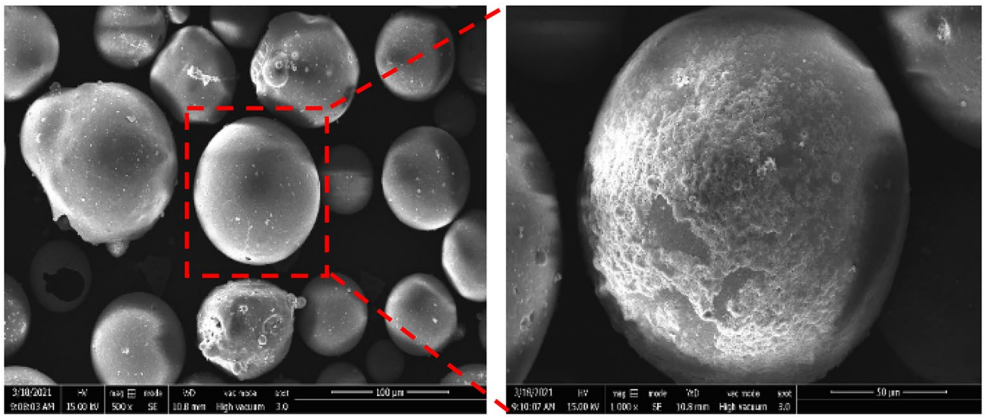

Figure 1 SEM micrograph of fly-ash cenospheres

Table 2 Formula of braking materials (mass fraction, %)

Composition	Fly-ash cenospheres	Resin	Coir fibre	Al_2O_3	$BaSO_4$	Rubber	Graphite
Content	0	20	10	20	42	5	3
	5				37		
	10				32		
	15				27		
	20				22		
	25				17		

Table 3 Design of orthogonal test (mass fraction, %)

List	1	2	3	4	5	6	7	8	9	10	11	12	13
Factor	A	B	A×B		C	A×C		D	A×D		Empty	Empty	Empty

Table 4 Level of orthogonal test (mass fraction, %)

Code	A	B	C	D
Factor	Fly-ash cenospheres	Resin	Coir fibre	Al_2O_3
Level				
1	10	10	5	10
2	15	15	7.5	15
3	20	20	10	20

this experiment, an L_{27} (3^{13}) orthogonal table was used, with the thread design shown in Table 3. A×B, A×C, and A×D represent the interactions between A and B, A and C, and A and D, respectively. For each factor, three levels were selected, as shown in Table 4.

The significance of the influence of each factor and their interaction on the experimental results was determined using analysis of variance. The specific calculation steps are as follows:

(1) Calculate the value of K_{ij}, which is the sum of the test results at level i in column j.

(2) Calculate the sum of the squared deviation S_j as follows:

$$S_j = \frac{r}{n}\sum_{i=1}^{r} K_{ij}^2 - \frac{1}{n}(\sum_{i=1}^{n} y_i)^2, \quad (1)$$

where r is the number of levels, n is the total number of experiments, and the test results are denoted as y_1, y_2, y_3,..., y_n. In this experiment, $r = 3$, and $n = 27$.

(3) Calculate the observed value of F using the following formula:

$$F_j = \frac{S_j / f_j}{S_{e\Delta} / f_{e\Delta}} \tag{2}$$

If $S_j / f_j < S_e / f_e$, S_j will be incorporated into the sum of squares of error S_e as a new sum of squares of error, while its degrees of freedom f_j will also be incorporated into f_e as a new error degrees of freedom $f_{e\Delta}$. Where $f_j = r - 1$, and $f_e = \sum f_{\text{Empty}}$.

(4) Use the following formula to determine the significance of the influence of the testing factors on the test results:

$$F_j = \frac{S_j / f_j}{S_{e\Delta} / f_{e\Delta}} \sim F(f_j, f_{e\Delta}) \tag{3}$$

If $F_j \geq F_{1\text{-}0.01}(f_j, f_{e\Delta})$, it is considered to be significant at the $\alpha = 0.01$ level, indicating that this factor has a highly significant influence on the test results and is recorded as "***". If $F_{1\text{-}0.01}(f_j, f_{e\Delta}) > F_j \geq F_{1\text{-}0.05}(f_j, f_{e\Delta})$, it is considered to be significant at the $\alpha = 0.05$ level, indicating that this factor has a significant influence on the test results and is recorded as "**". If $F_{1\text{-}0.05}(f_j, f_{e\Delta}) > F_j \geq F_{1\text{-}0.1}(f_j, f_{e\Delta})$, it is considered to be significant at the $\alpha = 0.10$ level, indicating that this factor has an influence on the test results and is recorded as "*". If $F_{1\text{-}0.1}(f_j, f_{e\Delta}) > F_j \geq F_{1\text{-}0.2}(f_j, f_{e\Delta})$, it is considered to be statistically significant at the $\alpha = 0.20$ level, indicating that this factor has a minor impact on the test results and is recorded as "Δ". If $F_j < F_{1\text{-}0.2}(f_j, f_{e\Delta})$, then at the significance level $\alpha = 0.20$, this factor is considered to have no influence on the test results.

2.2.3 Performance Characterization

The thermal stability of the material was tested using a NETZSCH model 449F5 synchronous thermal analyzer manufactured by in Germany. The test conditions include a powder mass of less than 20 mg, a test temperature range of 25–1000 °C, a heating rate of 10 °C/min, and a heating atmosphere of air.

According to the gas density measurement method outlined in the GB/T 24586-2009 standard, the true density of the braking materials was tested using a model 1340 true density meter. The hardness of the braking materials was tested using an XHRD-150 electric plastic Rockwell hardness tester. The diameter of the ball indenter used for the hardness test was 6.35 mm, the initial load was 98 N, and the total load was 980 N. The test process was conducted in accordance with the GB/T3398.2-2008 standard. The sample's impact strength was tested using a model XJJ-5 simple beam pendulum impact tester, following the experimental process outlined in the GB/T 1451-2005 standard. Sample size: 50 mm (± 1 mm) × 6 mm (± 0.5 mm) × 4 mm (± 0.2 mm). Repeat the measurement for each sample three times, and calculate the average value from the result.

The X-DM variable speed friction testing machine model was utilized to evaluate the macroscopic friction and wear characteristics of the braking materials. The temperature range is 100–350 °C, and the experiment is conducted at 50 °C intervals from 100 °C to 350 °C, resulting in a total of 6 groups. The testing process is conducted in accordance with the national standard GB5763-2008. The utomatically calculates the friction coefficient, measures the wear thickness using a micrometer, and calculates the volumetric wear rate.

The microscopic morphology and composition of the worn surface of the braking materials were analyzed using a model Quanta250 tungsten filament scanning electron microscope with a tungsten filament and an energy dispersive spectroscopy analyzer.

3 Results and Discussion

3.1 Effect of Fly-Ash Cenospheres on the Thermal Stability of Braking Materials

To investigate the impact of fly-ash cenospheres on the thermal stability of braking materials, thermal gravimetric analysis was performed on fly-ash cenospheres, braking materials without fly-ash cenospheres, and braking materials with 20% fly-ash cenospheres. The results are depicted in Figure 2. As illustrated in Figure 2(a), the hollow fly-ash cenospheres exhibit minimal mass loss from room temperature to 1000 °C in an air atmosphere, with a weight loss rate of only 0.92%. The DTG curve exhibits a minor endothermic peak in the temperature range of 80–120 °C, primarily attributed to the precipitation of water in the material's phase. There is a slight mass loss indicated on the TG curve, after which the material stabilizes without any significant weight loss. It is evident that the fly-ash cenospheres exhibit good thermal stability, and incorporating them into braking materials can enhance the thermal stability of the braking materials.

As depicted in Figures 2(b) and (c), the TG and DTG curves of the samples with and without 20% fly-ash cenospheres exhibit similarities. The weight loss process of the braking material can be roughly divided into three stages. The first stage occurs around 100 °C, and the weight loss rate of the material is approximately 0.35%. The weight loss during this stage is primarily caused by the release of adsorbed water and crystal water from certain raw materials, which corresponds to a small endothermic peak on the DSC curve. The second stage is the temperature interval of A (250–350 °C), during which a significant endothermic peak appears on the DTG curve, and the

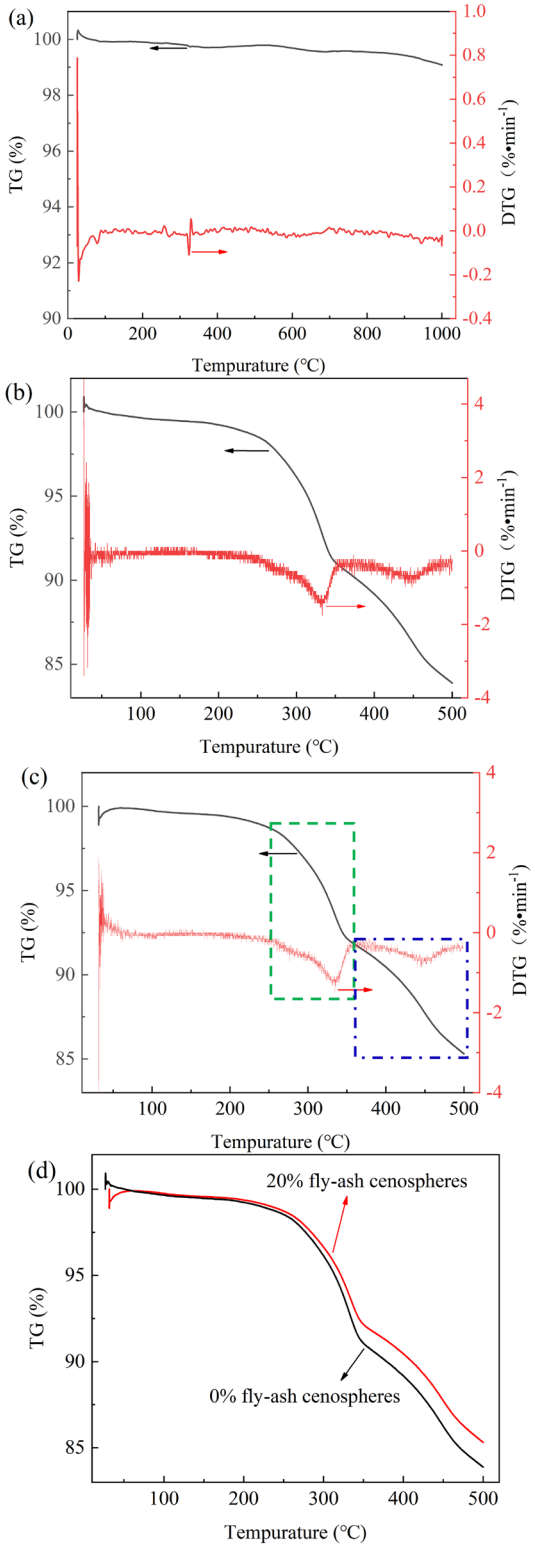

Figure 2 TG/DTG curves of fly-ash cenospheres and braking materials: (**a**) Fly-ash cenospheres, (**b**) Braking materials without fly-ash cenospheres, (**c**) Braking materials with 20% fly-ash cenospheres, (**d**) Comparison of thermogravimetry

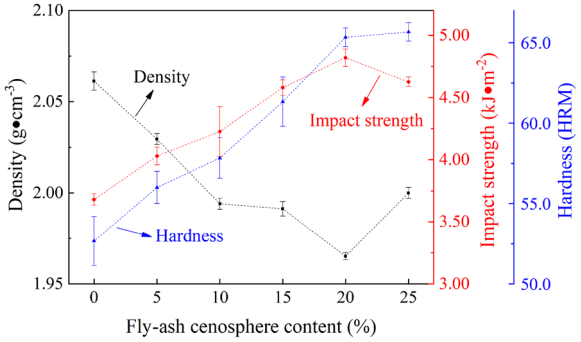

Figure 3 The density, hardness and impact strength of braking materials

material's weight loss accelerates, with a weight loss rate of 6.6%. This stage primarily involves heating and decomposing the cellulose, hemicellulose, and lignin in the resin and coir fiber. The third stage is a B temperature interval (250–500 °C), during which the material experiences a weight loss rate of 6.85%. This corresponds to a small endothermic peak on the DTG curve. The weight loss of materials in this stage mainly results from the carbonization and decomposition of resins and fibers. Figure 2(d) illustrates that while the thermal weight loss patterns of the two samples are similar, the weight loss rates at different stages vary. The thermal weight loss of the sample containing 20% fly-ash cenospheres at temperatures above 250 °C is lower than that of the sample containing no fly-ash cenospheres. The addition of fly-ash cenospheres to the braking materials can enhance the thermal stability of the composite material during the medium and high temperature stages.

3.2 Effect of Fly-Ash Cenospheres on the Density, Hardness, and Impact Strength of Braking Materials

The effect of different fly-ash cenospheres content on the density of the braking materials is illustrated in Figure 3. As depicted in Figure 3, the density of the sample initially decreases and then increases with the rise in the content of fly-ash cenospheres. The sample without fly-ash cenospheres has the highest density. Incorporating fly-ash cenospheres as a filler in the braking materials can effectively decrease the density of the composite material. Fly-ash cenospheres exhibit characteristics such as lightweight, hollow structure, and low density. Adding them to the braking materials can reduce the density of the composite material. As the content of fly-ash cenospheres increases, the density of the braking materials gradually decreases. When the cenospheres content is 20%, the density of the braking material reaches a minimum value of 1.97 g/cm^3. As the content of fly-ash

cenospheres increases, the cenospheres in the composite material gradually transition from the original dispersed arrangement in the resin to a tightly ordered accumulation form. This results in an increase in the density of the material.

The hardness of the braking materials increases with the higher content of cenospheres. The hardness of the sample without fly-ash cenospheres is the lowest, and the hardness of the sample containing 25% fly-ash cenospheres reaches a maximum of 65.7 HRM, which is 24% higher than that of the sample without fly-ash cenospheres. As shown in Table 1, primary constituents of fly-ash cenospheres are SiO_2 and Al_2O_3, both of which are materials known for their high hardness. Therefore, fly-ash cenospheres also exhibit high hardness. When the sample is compressed by external forces, the cenospheres dispersed throughout the sample can resist the penetration of external objects. As the content of cenospheres increases, their ability to resist pressure from hard objects on the surface strengthens, leading to an overall increase in the macroscopic hardness of the braking materials.

The impact strength of the braking material initially increased and then decreased with the increasing content of fly-ash cenospheres. The impact strength of the braking material containing 20% fly-ash cenospheres reached a maximum value of 4.63 kJ/m^2, while the impact strength of the sample without fly-ash cenospheres was 3.68 kJ/m^2, representing a 28.76% increase compared to the sample without fly-ash cenospheres. The fly-ash cenospheres are small, spherical particles with high strength and hardness. Cenospheres added to braking materials can disperse well within the matrix. According to the energy dissipation theory [27], the dispersed hollow particles can generate numerous small cracks within the composite material and absorb a significant amount of energy to hinder the propagation of these cracks, thereby effectively enhancing the toughness and strength of the composite material.

3.3 Effect of Fly-Ash Cenospheres on the Friction and Wear Performance of Braking Materials

A series of friction and wear performance tests were conducted on braking materials with varying levels of fly-ash cenospheres at temperatures ranging from 100 °C to 350 °C. The results of these tests are depicted in Figure 4. It can be observed from Figure 4(a) that the friction coefficient of braking materials without fly-ash cenospheres initially increases and then decreases with rising temperature, reaching a peak of 0.60 at 150 °C. In the temperature range of 300–350 °C, the friction coefficient of the sample decreases significantly, dropping below that at 100 °C. The inclusion of fly-ash

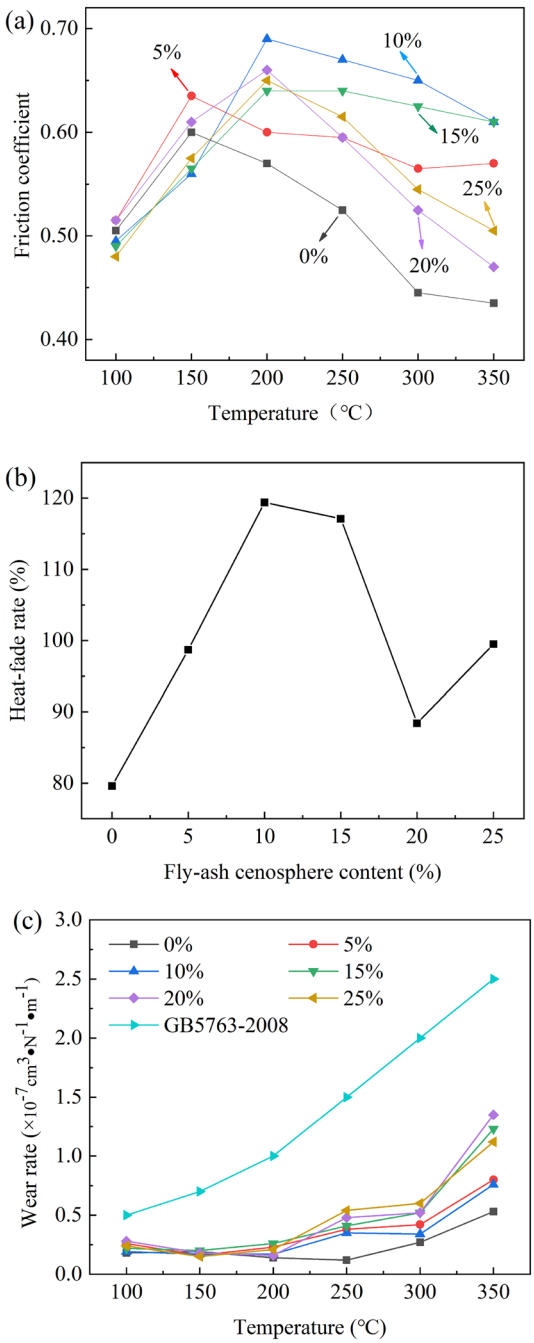

Figure 4 Friction and wear properties of braking materials: (**a**) Friction coefficient, (**b**) Heat-fade rate, (**c**) Wear rate

cenospheres significantly improved the friction coefficient of the braking material at temperatures ranging from 200 °C to 350 °C. Additionally, the friction coefficient at 300–350 °C remained higher than that at 100 °C. When the cenosphere content reached 20%, the friction coefficient of the sample decreased at 300–350 °C. The addition of fly-ash cenospheres to braking

materials has been shown to effectively increase the material's friction coefficient at moderate and high temperatures. This is primarily attributed to the excellent thermal stability of fly-ash cenospheres.

To compare the heat-fade resistance of fly-ash cenospheres in braking materials with varying levels of content, the thermal decay rate R is defined to characterize the heat-fade resistance of the sample's friction coefficient. The formula is as shown in Eq. (4):

$$R = \frac{\mu_{300-350}}{\mu_{100-150}} \times 100\%, \tag{4}$$

where $\mu_{300\text{-}350}$ is the average friction coefficient of the sample at 300–350 ℃. The average friction coefficient of the sample at 100–150 ℃ is $\mu_{100\text{-}150}$. A higher the R value indicates better the heat-fade resistance of the braking materials. R < 100% indicates that the coefficient of friction of the braking materials in high temperatures (300–350 ℃) is lower than that at low temperatures (100–150 ℃), suggesting thermal decay of the material. $R \geq 100\%$ indicates that the friction coefficient of the braking materials remains unchanged at high temperatures, demonstrating excellent heat-fade resistance. The heat-fade rate of the braking materials with varying fly-ash cenospheres content is depicted in Figure 4(b). As depicted in Figure 4(b), the incorporation of fly-ash cenospheres in braking materials can significantly enhance their heat-fade resistance. Braking materials containing 10% and 15% fly-ash cenospheres demonstrated the highest improvement.

As depicted in Figure 4(c), the wear rate of resin-based braking materials steadily increases with rising brake temperature. Moreover, the rate of wear exhibits a more pronounced increase at temperatures exceeding 250 °C. This is primarily because organic polymer materials, such as phenolic resin and natural fiber in resin-based braking materials, start to undergo thermal decomposition and carbonization at temperatures exceeding 250 °C, leading to an increase in the wear rate. The inclusion of fly-ash cenospheres in the braking materials has minimal effect on the wear rate of the sample at 100–200 °C, but it increases the wear rate of the braking materials at 250–350 °C. Compared to the specifications for the fourth type of disc brake lining in the national standard for disc brake linings (GB5763-2008), the wear rate of braking materials containing fly-ash cenospheres remains at a relatively low level, indicating excellent wear resistance.

3.4 Wear Mechanism of Fly-Ash Cenospheres Filled Braking Materials

To further investigate the influence of fly-ash cenospheres on the wear characteristics of resin-based braking materials, the wear surfaces of braking materials with and without 10% fly-ash cenospheres were observed and analyzed after friction and wear tests at temperatures of 100 °C, 250 °C, and 350 °C. The results are presented in

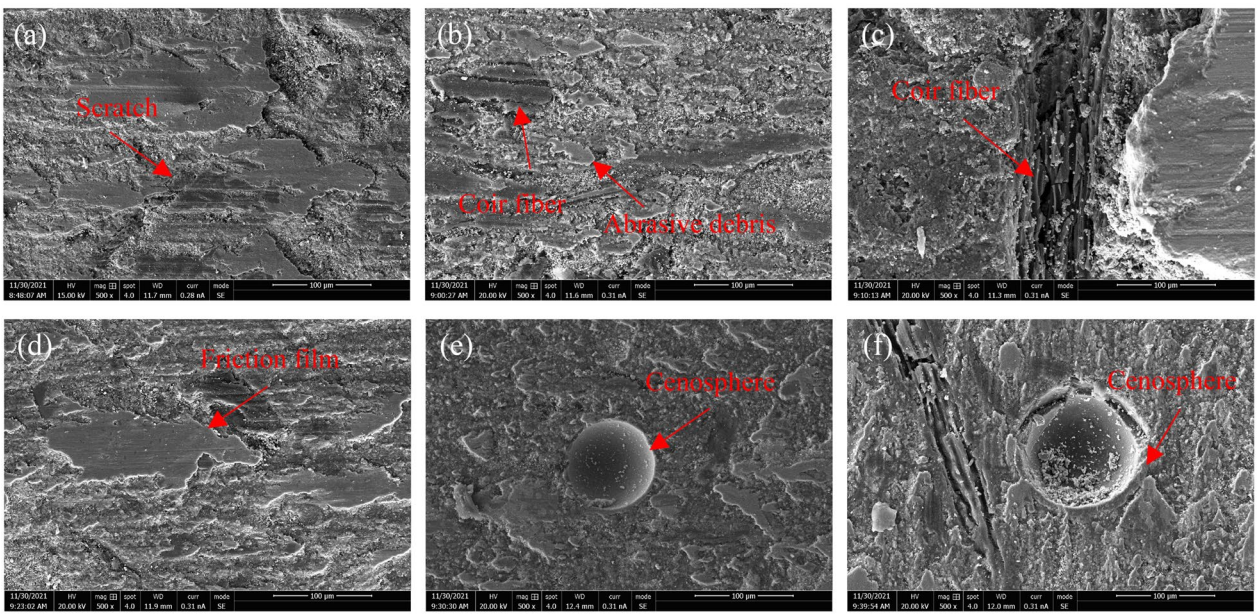

Figure 5 Wear morphology of braking materials at different temperatures: (**a**) 0%-100 ℃, (**b**) 0%-250 ℃, (**c**) 0%-350 ℃, (**d**) 10%-100 ℃, (**e**) 10%-250 ℃, (**f**) 10%-350 ℃

Figure 5. As depicted in Figure 5(a), at a braking temperature of 100 °C, the friction surface integrity of the sample without fly-ash cenospheres exhibits good integrity, with no visible cracks or peeling pits, and some scratches are clearly evident on the surface. The scratching on the friction surface is primarily caused by two factors. Firstly, during the friction process, the micro-convex bodies on the surface of the brake disc create a ploughing action on the surface of the braking materials under the load, leading to scratches on the sample surface. Secondly, the abrasive particles produced during friction contain high-hardness fillers, and some of these particles with high hardness are present between the contact surfaces of the braking materials and the mating component, resulting in three-body abrasive wear. At present, the primary form of wear on the braking material is abrasive wear. As depicted in Figure 5(d), at a braking temperature of 100 °C, the brake material containing 10% fly-ash cenospheres also exhibits good surface integrity. In comparison to Figure 5(a), a blocky friction film starts to emerge on the surface layer of the sample. At present, the predominant form of wear on the braking material is a combination of abrasive wear and adhesive wear.

As depicted in Figure 5(b), at a braking temperature of 250 °C, a significant quantity of wear debris and some exposed coir fiber can be observed on the friction surface of the braking materials without fly-ash cenospheres. This is because resin-based braking materials contain a significant amount of organic components, particularly phenolic resins, which undergo viscous flow decomposition under mechanochemical action during high-temperature friction. The tar-like substances formed during decomposition decrease the friction coefficient of the braking materials, resulting in thermal degradation [28, 29]. The thermal decomposition of certain resin layers on the surface weakens their bonding effect on other components, leading to the exposure of fibers, shedding of some fillers, and the generation of a significant amount of abrasive debris. This results in an increased in wear rate of the sample. The primary cause of wear on the braking material is thermal degradation of the resin. As shown in Figure 5(f), at 250 °C, the braking materials containing 10% fly-ash cenospheres still has a relatively smooth surface, and a more consistent and continuous friction film is present on the sample's surface. The friction film forms and covers the friction surface during the friction and wear process, becoming the primary contact area between the braking materials and the brake disc. This phenomenon is beneficial for the friction performance of the braking materials [11, 30]. This is primarily attributed to the inclusion of fly-ash cenospheres, which aid in the formation of a friction film on the surface of the braking materials. Additionally, its excellent thermal stability delays the thermal decomposition of the resin to a certain extent, thereby suppressing the thermal degradation behavior of the braking materials. The primary form of wear for braking materials is adhesive wear.

As shown in Figure 5(c), at 350 °C, some of the resin and coir fiber on the friction surface of the braking materials without fly-ash cenospheres have undergone carbonization, and some of the fibers and filler have detached, forming large pits on the surface. The friction coefficient of the sample decreases, and the wear rate increases, which is attributed to significant thermal degradation. At this point, the wear of the braking material is caused by the carbonization of the organic polymer material. As depicted in Figure 5(f), the surface of the braking materials containing 10% fly-ash cenospheres remained smooth, and some friction film could still be observed. However, the fiber component of the sample surface began to carbonize, the fly-ash cenospheres started to wear, and the surface debris also began to increase. Consequently, this led to a decrease in the friction coefficient and an increase in the wear rate of the braking materials. The primary forms of wear of braking materials are adhesive wear and wear caused by the carbonization of organic polymers.

To further investigate the elemental distribution on the wear surface of resin-based braking materials filled with fly-ash cenospheres, the surface of braking materials containing 10% fly-ash cenospheres was analyzed using energy spectrum technology after a 350 °C friction and wear test, as shown in Figure 6. The sample's surface is primarily composed elements such as C, O, Al, Si, Fe, and Ba. Through analysis of the circular region on the surface of the sample, it was determined that the main components were Al, Si, and O. This indicates that the area was left behind when the fly-ash cenospheres were worn away. The friction film on the surface and some wear debris contain Fe, which was transferred from the brake disc to the sample surface during the braking process. This further indicates that the friction film formed and covering the friction surface during the friction and wear process becomes the main contact area between the braking materials and the counterpart. Additionally, the friction film also contains Al, Si, and O elements, with a composition corresponding to that of the fly-ash cenospheres. This finding further confirms that the inclusion of fly-ash cenospheres contributes to the formation of the friction film on the surface of the braking material during the friction and wear process.

3.5 Formula Optimization

The results of the orthogonal experiment variance analysis for the orthogonal test reveal the effects of the factors

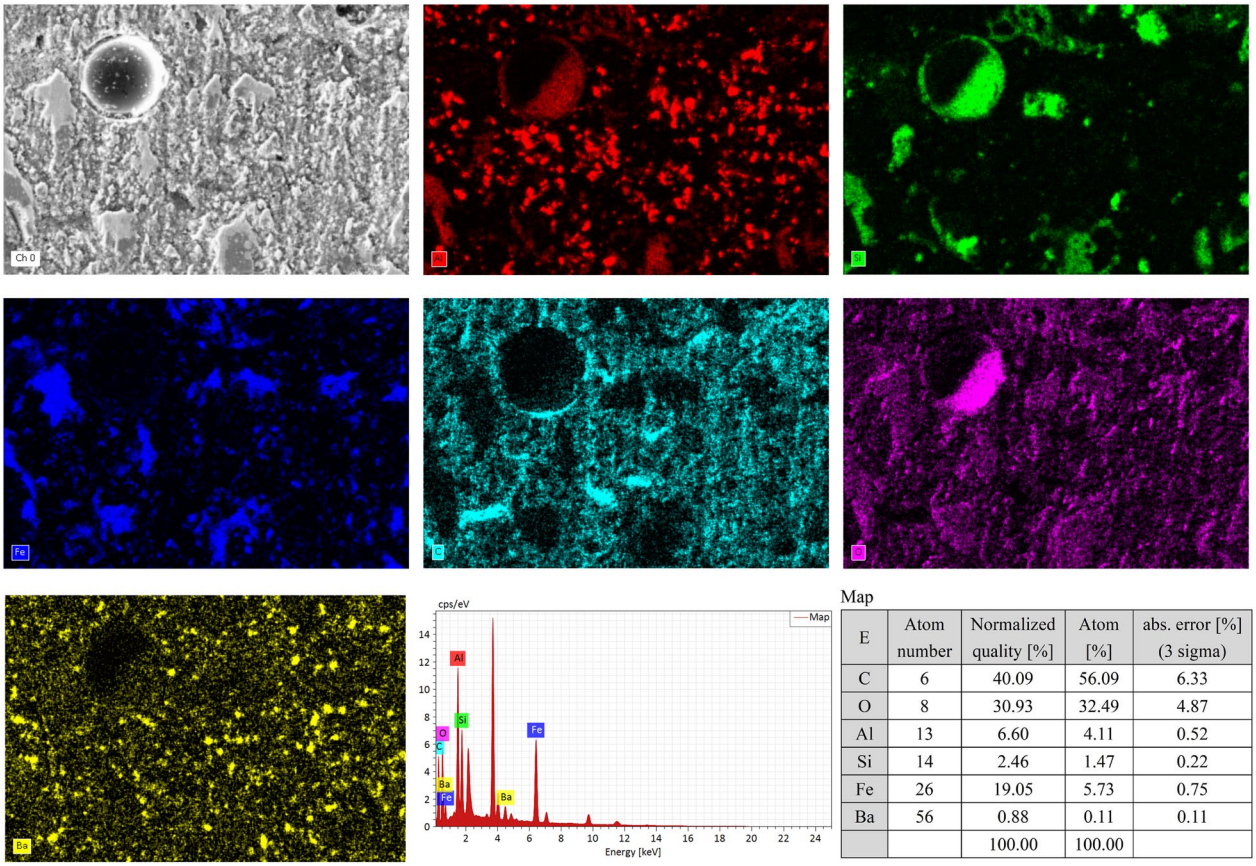

Map

E	Atom number	Normalized quality [%]	Atom [%]	abs. error [%] (3 sigma)
C	6	40.09	56.09	6.33
O	8	30.93	32.49	4.87
Al	13	6.60	4.11	0.52
Si	14	2.46	1.47	0.22
Fe	26	19.05	5.73	0.75
Ba	56	0.88	0.11	0.11
		100.00	100.00	

Figure 6 EDS analysis for wear surface of braking materials filled with fly-ash cenospheres

Table 5 Effect of the factors and their interactions on the friction coefficient

Temperature (℃)	**100**	**150**	**200**	**250**	**300**	**350**
Significance	A***	A***	A×B*	B*	A***	A**
	B**	B***	C△	D***	B***	B**
	A×B△	A×B*	A×C△		A×B*	A×B**
	C△		D**		D***	C*
	A×D△					A×C△

Table 6 Effect of the factors and their interactions on the wear rate

Temperature (℃)	**100**	**150**	**200**	**250**	**300**	**350**
Significance	B△	A△	A**	A**	A***	A*
	A×D△	B***	B***	B***	B***	B***
		A×B△		A×B△	C△	A×B**
		A×C△		C**	D***	C△
		D△		D△		A×C△
						D△
						A×D△

Table 7 Optimum formulation of braking materials (mass, %)

Component	Cenospheres	Resin	Fiber	Al_2O_3	$BaSO_4$	Rubber powder	Granite
Content	20	15	10	15	32	5	3

Table 8 Test results of optimum formulation of braking materials

Optimum formulation	Test temperature					
	100 ℃	**150** ℃	**200** ℃	**250** ℃	**300** ℃	**350** ℃
Friction coefficient (μ)	0.60	0.58	0.59	0.60	0.57	0.61
Wear rate ($\times 10^{-7}$ $cm^3 \cdot N^{-1} \cdot m^{-1}$)	0.29	0.34	0.48	0.52	0.56	0.65

and their interactions on the friction coefficient and wear rate, as presented in Tables 5 and 6. Among them, "***" represents a highly significant influence, "**" represents a significant influence, "*" represents an influence, and Δ represents a minor impact.

As depicted in Table 5, it is evident that within the low-temperature range of 100–150 °C, the effect of fly-ash cenospheres content on the friction coefficient of the specimen is highly significant, followed by the impact of resin content. The friction coefficient of the braking materials is slightly influenced by the coir fibers content, the interaction between resin and cenospheres, and the interaction between Al_2O_3 and cenospheres. At 200–250 °C, the primary factor contributing to the improvement of the friction coefficient of the sample is Al_2O_3. The resin content and the interaction between the fly-ash cenospheres and the resin have a slight influence on the friction coefficient of the sample. However, the coir fiber content and the interaction between fly-ash cenospheres and coir fibers have little influence on the friction coefficient of the sample. At 300–350 °C, the effect of fly-ash cenospheres content and resin content on the friction coefficient of the specimen is most significant. The interaction between resin and cenospheres significantly influences on the friction coefficient of the sample. Overall, the primary factors influencing the friction coefficient of the samples are cenospheres, resins, and Al_2O_3.

As shown in Table 6, at 100–150 ℃, the resin content has a significant effect on the wear rate of the sample, while the other components have little impact on the wear rate of the sample. At 200–250 °C, the resin content has the most significant influence on the sample's wear rate, followed by the cenospheres content. During the high-temperature stage (300–350 °C), the resin content has the most significant influence on the wear rate of the sample, followed by the cenospheres content. It is evident that the factors that the cenospheres and resin content are the significant factors affecting the wear rate of the sample.

Aiming to enhance the high-temperature friction and wear performance of braking materials and based on the analysis of orthogonal experiment results, the optimized formula for braking materials was obtained, as shown in Table 7. The friction and wear test results are presented in Table 8. As indicated in Table 8, within the temperature range of 100–350 ℃, the optimized formula exhibits a friction coefficient of 0.57–0.61 and a wear rate of (0.29–0.65) $\times 10^{-7}$ $cm^3 \cdot N^{-1} \cdot m^{-1}$, indicating excellent heat-fade resistance and stability of the friction coefficient.

4 Conclusions

(1) The addition of fly-ash cenospheres to the braking materials enhances the thermal stability of the composite material at medium and high temperatures. The density of the composite material initially decreases and then increases as the content of fly-ash cenospheres increases, while the hardness increases with the increase of fly-ash cenospheres. The impact strength initially increases and then decreases with the increase of fly-ash cenospheres.

(2) The inclusion of fly-ash cenospheres in braking materials can substantially enhance the friction coefficient at moderate and high temperatures (200–350 °C), effectively improving the heat-fade resistance of the braking materials.

(3) The main type of wear for braking materials without fly-ash cenospheres is abrasive wear at low and medium temperatures. At elevated temperatures, the primary cause of wear is thermal degradation and carbonization of the resin. The incorporation of fly-ash cenospheres improves the formation of surface friction films during the friction and wear pro-

cess of braking materials, promoting the transition from abrasive wear to adhesive wear.

(4) The optimal formulation of the resin-based braking material filled with fly-ash cenospheres is as follows: 20% cenospheres, 15% resin, 10% Coir fiber, 15% Al_2O_3, 32% $BaSO_4$, 5% rubber powder, and 3% graphite. At 100–350 ℃, the friction coefficient of the optimal formulation ranges from 0.57 to 0.61, and the wear rate ranges from 0.29×10^{-7} to 0.65×10^{-7} $cm^3{\cdot}N^{-1}{\cdot}m^{-1}$, demonstrating excellent resistance to heat-fade and stability in friction coefficient.

Acknowledgements
Not applicable.

Authors' Contributions
KZ and YL conceived and designed the experiments; SY performed the experiments; KZ, YL and SY analyzed the data; KZ, YL, SY, ZR and JH wrote the manuscript. All authors read and approved the final manuscript.

Funding
Supported by National Natural Science Foundation of China (Grant No. 52275178), Fujian Provincial Natural Science Foundation of China (Grant Nos. 2020J05115, 2022J01073), and Project National United Engineering Laboratory for Advanced Bearing Tribology, Henan University of Science and Technology of China (Grant No. 202103).

Declarations

Competing Interests
The authors declare no competing financial interests.

Received: 11 September 2023 Revised: 2 February 2024 Accepted: 23 February 2024
Published online: 20 March 2024

References

[1] V Chauhan, J Bijwe, A Darpe. Functionalization of Al2O3 particles to improve the performance of eco-friendly brake-pads. *Friction*, 2021, 9(5): 1213-1226.
[2] R Tavangar, H A Moghadam, A Khavandi, et al. Comparison of dry sliding behavior and wear mechanism of low metallic and copper-free brake pads. *Tribology International*, 2020, 151: 106416.
[3] Y L Xiao, Y Cheng, H P Zhao, et al. Airborne brake wear particle emissions: A review. *Tribology*, 2022, 42(6): 1290-1304. (in Chinese)
[4] M Liu, D Y Hou, K K Zheng, et al. Characterization of friction and wear of phenolic resin matrix composites reinforced by bamboo fibers of alkaline and LaCl3 treatment. *Materials Today Communications*, 2023, 35: 106361.
[5] K K Zheng, C H Gao, F S He, et al. Development of a high-quality rare earth oxide modified resin-based brake material. *Tribology - Materials, Surfaces & Interfaces*, 2019, 13(1): 50-57.
[6] J S Qu, W J Wang, Z Y Dong, et al. Simulation analysis and verification of temperature and stress of wheel-mounted brake disc of a high-speed train. *Chinese Journal of Mechanical Engineering*, 2022, 35: 99.
[7] G Straffelini, R Ciudin, A Ciotti, et al. Present knowledge and perspectives on the role of copper in brake materials and related environmental issues: A critical assessment. *Environmental Pollution*, 2015, 207: 211–219.
[8] Z Y Fan , Z Y Xiang, J L Mo, et al. Effect of filling materials into friction block on brake performance of high-speed train brake pad. *Tribology*, 2022, 42(5): 900-912. (in Chinese)
[9] M Leonardi , M Alemani, G Straffelini, et al. A pin-on-disc study on the dry sliding behavior of a Cu-free friction material containing different types of natural graphite. *Wear*, 2020, 442: 203157.
[10] K K Zheng, C H Gao, F S He, et al. The role of rare earth lanthanum oxide in polymeric matrix brake composites to replace copper. *Polymers*, 2018, 10(9): 1027.
[11] L Y Barros, J C Poletto, P D Neis, et al. Influence of copper on automotive brake performance. *Wear*, 2019, 426: 741-749.
[12] N Kalel, B Bhatt, A Darpe, et al. Copper-free brake-pads: A break-through by selection of the right kind of stainless steel particles. *Wear*, 2021, 464: 203537.
[13] V Mahale, J Bijwe, S Sinha. A step towards replacing copper in brake-pads by using stainless steel swarf. *Wear*, 2019, 424: 133-142.
[14] K Yu, X Shang, X G Zhao, et al. High frictional stability of braking material reinforced by basalt fibers. *Tribology International*, 2023, 178: 108048.
[15] N Aranganathan, J Bijwe. Comparative performance evaluation of NAO friction materials containing natural graphite and thermo-graphite. *Wear*, 2016, 358: 17-22.
[16] H Yu Lin, H Z Cheng, K J Lee, et al. Effect of carbonaceous components on tribological properties of copper-free NAO friction material. *Materials*, 2020, 13(5): 1163.
[17] V Mahale, J Bijwe, S Sinha. Efforts towards green friction materials. *Tribology International*, 2019, 136: 196-206.
[18] C Menapace, M Leonardi, V Matějka, et al. Dry sliding behavior and friction layer formation in copper-free barite containing friction materials. *Wear*, 2018, 398: 191-200.
[19] L Wei, Y S Choy, C S Cheung, et al. Tribology performance, airborne particle emissions and brake squeal noise of copper-free friction materials. *Wear*, 2020: 203215.
[20] K K Zheng, Y X Lin, T Z Lai, et al. Replacing copper in composites with waste foundry sand: A novel approach for Cu-free resin-based braking material. *Tribology International*, 2024, 191: 109110.
[21] D Sunjidmaa, G Batdemberel, S Takibai. A study of ferrospheres in the coal fly ash. *Open Journal of Applied Sciences*, 2019, 9(1): 10.
[22] J Q Wu, Z H Lu, Y T Chen, et al. Mechanical properties and cracking behaviour of lightweight engineered geopolymer composites with fly ash cenospheres. *Construction and Building Materials*, 2023, 400: 132622.
[23] E Grabias-Blicharz, W Franus. A critical review on mechanochemical processing of fly ash and fly ash-derived materials. *Science of the Total Environment*, 2023, 860: 160529.
[24] F W Zhang, K K Zheng, Y X Lin, et al. Effect of particle sizes of fly-ash cenospheres on the mechanical and tribological properties of resin-based composites. *Lubrication Engineering*, 2022, 47(11): 27-32.
[25] A Nithyanandam, T Deivarajan. Development of fly ash cenosphere-based composite for thermal insulation application. *International Journal of Applied Ceramic Technology*, 2021, 18(5): 1825-1831.
[26] J C Li, P Chen, Y Wang. Tribological and corrosion performance of epoxy resin composite coatings reinforced with graphene oxide and fly ash cenospheres. *Journal of Applied Polymer Science*, 2021, 138(11): 50042.
[27] M Z Wang, Z G Shen, Y H Zheng, et al. In situ observation and analysis on cenosphere/PP composite under the tensile test. *Acta Materiae Compositae Sinica*, 2007(4): 51-57.
[28] J Bijwe, N N Majumdar, B K Satapathy, et al. Influence of modified phenolic resins on the fade and recovery behavior of friction materials. *Wear*, 2005, 259(7-12): 1068-1078.
[29] K K Zheng, C H Gao, F S He, et al. Study on the interfacial functionary mechanism of rare-earth-solution-modified bamboo-fiber-reinforced resin matrix composites. *Materials*, 2018, 11(7): 1190.
[30] P Zhang, L Zhang, P F Wu, et al. The multi-scale strengthened friction film eable braking performance of copper-based brake pad in high-speed emergency braking. *Tribology Transactions*, 2023, 66(3): 519-529.

Kaikui Zheng born in 1986, is currently a professor and a PhD candidate supervisor at *School of Mechanical Engineering and Automation, Fuzhou University, China*. His main research interests include tribology, surface Engineering, and additive manufacturing.

Youxi Lin born in 1967, currently a professor and a PhD candidate supervisor at *School of Mechanical Engineering and Automation,*

Fuzhou University, China. His main research interests include mechanical engineering and advanced manufacturing technology.

Shanmin You born in 1996, is a master candidate at *School of Mechanical Engineering and Automation, Fuzhou University, China*.

Zhiying Ren born in 1980, currently a professor and a PhD candidate supervisor at *School of Mechanical Engineering and Automation, Fuzhou University, China*. Her main research interests include tribology, metal rubber, and vibration noise.

Jianmeng Huang born in 1973, currently a professor and a master candidate supervisor at *School of Mechanical Engineering and Automation, Fuzhou University, China*. His main research interests include tribology and mechanical design.